Atypical endo-β-1,4-mannannases are necessary for normal glucomannan synthesis in Arabidopsis

Aina Kikuchi[a,1], Eriko Sato[a,1], Yoshihisa Yoshimi[b], Hironori Takasaki[a], Naho Nishigaki[a], Kimie Atsuzawa[c], Yasuko Kaneko[d], Masatoshi Yamaguchi[a], Daisuke Takahashi[a], Paul Dupree[b], and Toshihisa Kotake[a,e,2]

Author affiliations: [a]Graduate School of Science and Engineering, Saitama University, 255 Shimo-Okubo, Sakura-ku, Saitama 338-8570, Japan; [b]Department of Biochemistry, University of Cambridge, Hopkins Building, The Downing Site, Tennis Court Road, Cambridge CB2 1QW, UK; [c]Comprehensive Analysis Center for Science, Saitama University, Saitama 338-8570, Japan; [d]Faculty of Education, Saitama University, 255 Shimo-Okubo, Sakura-ku, Saitama 338-8570, Japan; and [e]Green Bioscience Research Center, Saitama University, 255 Shimo-Okubo, Sakura-ku, Saitama 338-8570, Japan

[1] A.K. and E.S. contributed equally to this work.

[2] To whom correspondence may be addressed. Email: kotake@mail.saitama-u.ac.jp.

Type of manuscript: Research Article

Research area: Biological Sciences, Plant Biology

Corresponding author

Name: Toshihisa Kotake

Address: Division of Life Science, Graduate School of Science and Engineering, Saitama University, 255 Shimo-okubo, Sakura-ku, Saitama 338-8570, Japan

Phone: +81-48-858-3955

E-mail: kotake@mail.saitama-u.ac.jp

Keywords:

endo-β-1,4-mannanase, glucomannan, Golgi apparatus, membrane-anchored enzyme, vacuole transport

ABSTRACT

The molecular mechanisms underlying the synthesis and secretion of large cell wall polysaccharides in plant cells are not fully understood. In this study, we report that two atypical endo-β-1,4-mannanases (MANs), which are not secreted and do not degrade glucomannan in the cell wall, play a novel role in glucomannan synthesis. Among the six MANs in Arabidopsis, AtMAN2 and AtMAN5 contain a transmembrane (TM) domain at their N-terminal region instead of a signal peptide. Subcellular localization using MAN protein fused with fluorescent protein demonstrated that AtMAN2 localizes to the Golgi apparatus in vascular and interfascicular fiber cells. We found that an Arabidopsis *man2 man5* double mutant lost 65% of glucomannan in the cell walls of the inflorescence stem. Immunostaining revealed that the double mutant retained a small amount of glucomannan in the vacuole instead of secreting it to the cell walls. Arabidopsis possesses another atypical MAN, AtMAN6, with an HDEL retention signal at its C-terminus. However, mutation of AtMAN6 did not affect glucomannan content in the cell walls, suggesting distinct functions for these MANs. This study revealed that the function of AtMAN2 and AtMAN5 is necessary for normal glucomannan synthesis. We suggest that these *man* mutants point to an uncharacterized transport pathway in plant cells, through which glucomannan is trafficked to the vacuole instead of the cell walls.

54 **SIGNIFICANCE STATEMENT**

55 Cell wall polysaccharides are synthesized from building block nucleotide sugars by the
56 action of glucosyltransferases, but other factors facilitating the synthesis and secretion of
57 large polysaccharides without aggregation remain to be identified. Here, we focused on
58 the importance and functions of two atypical Arabidopsis endo-β-1,4-mannanases that
59 have a transmembrane domain instead of a secretion signal, and which are widely
60 distributed in angiosperms but have not been well characterized. Arabidopsis mutants
61 impaired in these endo-β-1,4-mannanases lost 65% cell wall glucomannan, indicating that
62 the hydrolysis by these enzymes is necessary for normal synthesis. Enhanced retention of
63 glucomannan inside cells in the mutant hints at a transport route to deliver glucomannan
64 to the vacuole.

65

66 **INTRODUCTION**

67 Plant cell wall polysaccharides constitute the largest biomass carbon reservoir on earth,
68 thus understanding the mechanism for their synthesis is indispensable for their efficient
69 production and utilization (1). Large polysaccharides are synthesized by
70 glycosyltransferases from building block nucleotide sugars (2), but its molecular
71 mechanism has not been fully understood. It is well-known that proteins undergo quality
72 control in which unfolded proteins are removed from the endoplasmic reticulum (ER) and
73 degraded by 26S proteasome in the cytosol (3). On the other hand, how aggregation of
74 large cell wall polysaccharides is avoided during the synthesis and how they are processed
75 if they do aggregate in plant cells are still unknown.

76 Mannan polysaccharides are cell wall polysaccharides widely distributed in land plants.
77 They commonly possess a backbone composed of β-1,4-mannose (β-1,4-Man) and/or β-
78 1,4-glucose (β-1,4-Glc), while the backbone sequences and decorations are diverse (4-6).
79 The backbones of mannan polysaccharides can take on a two-fold structure, in which the
80 sugar residues turn at 180° resulting in a straight ribbon structure suitable for cellulose
81 binding (7, 8). Mannan polysaccharides without decoration tend to become insoluble,
82 probably as a result of intermolecular hydrogen bonding and hydrophobic interaction (9,
83 10).

84 The backbones of mannan polysaccharides are synthesized from GDP-Man and GDP-
85 Glc by the action of specific glycosyltransferases, called cellulose-synthase like A (CslA)
86 proteins (11, 12, 13). In Arabidopsis (*Arabidopsis thaliana*), CslA2 synthesizes the
87 backbone for β-galactoglucomannan (β-GGM) with alternating β-1,4-Man and β-1,4-Glc

88 residues, whereas ClsA9 makes the backbone for acetylated GGM (AcGGM) with a
89 random sequence of β-1,4-Man and β-1,4-Glc residues (in the following parts,
90 glucomannan includes β-GGM and AcGGM) (7, 8, 14). Supporting the importance of
91 factors involved in the building block generation and the backbone synthesis reactions,
92 Arabidopsis *vitamin c defective1*, *konjac1*, *csla2, and csla9* mutants exhibit a decrease in
93 glucomannan content (12, 14-16). Subsequently, the backbones undergo decoration with
94 α-galactose by mannan α-galactosyltransferase and/or acetyl groups by mannan *O*-
95 acetyltransferase, with which the solubility of glucomannan increases (6, 17-19).
96 MANNAN SYNTHESIS-RELATED (MSR) proteins are other factors shown to affect
97 the glucomannan content, although their molecular functions are still obscure (20). The
98 identification of additional factors is important for understanding the molecular
99 mechanism of glucomannan synthesis and secretion.

100 Endo-β-1,4-mannanase (MAN) is one of the conserved cell wall enzymes in plants,
101 belonging to the glycoside hydrolase 5 family (21). The physiological importance of
102 MANs have been extensively studied in seed germination and fruit ripening (22, 23).
103 Based on the domains, motifs, and sequence similarity, plant MANs may be classified
104 into several types (Fig. 1A) (24). Arabidopsis secreted type MANs, AtMAN3 and
105 AtMAN7, hydrolyze cell wall glucomannan to contribute to cadmium-tolerance via
106 activation of phytochelatin and glutathione synthesis (25, 26). AtMAN6 is a HDEL-type
107 MAN with a C-terminal HDEL signal, which is a retrograde transport signal back from
108 the Golgi apparatus to the ER (27). AtMAN6 and its poplar (*Populus trichocarpa*)
109 orthologue, PtrMAN6, are specifically localized in vessel cells and presumed to release

110 GGM oligosaccharides as signaling molecules, which negatively regulate secondary cell
111 wall formation in the vessel and interfascicular fiber cells (28, 29). On the other hand,
112 AtMAN2 and AtMAN5 are the other type of MANs with a transmembrane (TM) domain
113 instead of a signal peptide in the N-terminal region, designated TM-type MANs here.
114 Recombinant AtMAN2 expressed in *Escherichia coli* shows hydrolytic activity toward
115 mannan polysaccharides and lacks transglycosylation activity (30), but its physiological
116 importance and functions remain to be studied.

117 This study focused on the importance and functions of the TM-type MANs, AtMAN2
118 and AtMAN5, comparing them with another atypical MAN, AtMAN6, in glucomannan
119 synthesis and secretion. The analysis of Arabidopsis loss-of-function mutants showed that
120 AtMAN2 and AtMAN5 are necessary for normal glucomannan synthesis, and in this
121 respect different from AtMAN6. We found that the impairment of normal synthesis was
122 accompanied by retention of relatively large glucomannan aggregates in the vacuole.
123 These findings provide new insights into the synthesis and secretion of plant cell wall
124 polysaccharides.

125

126 **RESULTS**

127 **TM-type MANs are conserved in angiosperms**

128 In Arabidopsis, two TM-type MANs, AtMAN2 (AT2G20680) and AtMAN5
129 (AT4G28320), are highly related in their amino acid sequences (identity, 83%), while
130 AtMAN6 (AT5G01930) is the sole HDEL-type MAN (Fig. 1A). TM-type MANs can be
131 found in other angiosperms including amborella (*Amborella trichopoda*) and rice (*Oryza*

132 *sativa*), forming a clade apart from the secreted type MANs in the phylogenetic tree (Fig.
133 1B). On the other hand, *Physcomitrium patens* (a moss species) and *Marchantia*
134 *polymorpha* (a liverwort species) lack this type. The HDEL-type MANs also formed a
135 different clade, which did not include MANs from *P. patens* and *M. polymorpha*. The
136 distribution and phylogenetic relationships suggest that the TM-type MANs have
137 functions differently from the secreted and the HDEL-type MANs.
138
139 **Loss of glucomannan in *man2 man5* double mutants**
140 To examine the importance of AtMAN2 and AtMAN5 and differentiate their role from
141 AtMAN6, we analyzed the glucomannan content of an Arabidopsis *man2-1 man5-1*
142 double mutant and compared it with the wild-type plant (WT), *man6-1*, and *man2-1*
143 *man5-1 man6-1* and *man2-2 man5-1 man6-1* triple mutants. These mutants did not show
144 significant growth defects (Fig. S1). Based on their expression patterns (Fig. S2) (31), the
145 changes in cell walls from the bottom part of inflorescence stems where secondary cell
146 wall thickening occurs, were analyzed. The cell walls were fractionated into water soluble
147 fraction (soluble fraction), alkali extractable fraction (alkali fraction), and cellulose
148 fractions (Fig. 2A), and the sugar composition of these fractions was determined by high-
149 performance anion-exchange chromatography with pulsed amperometric detection
150 (HPAEC-PAD) (Fig. S3). Although MANs are hydrolytic enzymes acting on mannan
151 polysaccharides (30), the *man2-1 man5-1* double mutant unexpectedly lost more than
152 65% mannose in these cell wall fractions (Fig. 2B). As other hemicelluloses and pectin
153 rarely have mannose residues in Arabidopsis (4, 14, 32), this result indicates that the

154 double mutant lost a large part of its glucomannan. It has been reported that AtMAN6
155 negatively regulates secondary cell wall thickening (29), but neither mannose content nor
156 the sugar content proportion of cell wall fractions was changed in the *man6-1* mutant.
157 The Arabidopsis inflorescence stem has two different glucomannans, β-GGM and
158 AcGGM, which are synthesized by CslA2 and CslA9, respectively (7, 8, 14). The
159 influence of the loss of TM-type MANs on these GGMs was evaluated by polysaccharide
160 analysis using carbohydrate gel electrophoresis (PACE) (Fig. S4). Here, β-GGM and
161 AcGGM included in the stem cell walls were hydrolyzed into oligosaccharides by a
162 microbial MAN, CjMAN26A, separated, and detected. The *man2-1 man5-1* double and
163 the triple mutants with *man6* showed almost no GBGAGM and GBGM oligosaccharides
164 from β-GGM and no GGM and GMM from AcGGM, so they were similar to the *csla2-2*
165 *csla9-2* double mutant in this respect (14) (Fig. 2C, S4). These results demonstrate that
166 the TM-type MANs are necessary for the normal synthesis of both β-GGM and AcGGM
167 in the inflorescence stem. The results also suggested that AtMAN2 and AtMAN5 function
168 redundantly for the glucomannan synthesis.
169
170 **Retention of glucomannan in the vacuole**
171 The change in the accumulation of glucomannan in vascular and interfascicular fiber cells
172 in *man* mutants was also observed in cross-sections of inflorescence stems. The
173 glucomannan localized in these cells was detected with LM21 antibody specific to
174 glucomannan. Consistent with the results of the cell wall analysis (Fig. 2), the cell wall
175 glucomannan signals were almost lost in the *man2-1 man5-1* double and the triple mutants

176 (Fig. 3A). Xylan, together with cellulose, is a major component of secondary cell walls,
177 but neither immunostaining of xylan nor the sugar composition of cell wall fractions (Fig.
178 S5) pointed to compensatory changes in the mutants. The TM-type MANs do not seem
179 to influence the content of other cell wall polysaccharides in the inflorescence stem.

180 The *man2-1 man5-1* double mutant lost cell wall glucomannan but instead showed the
181 glucomannan signals inside cells (Fig. 3B). Given that the double mutant is impaired in
182 the synthesis of glucomannan, the intracellular signals are presumed to stem from a small
183 amount of glucomannan that aggregated influencing the synthesis and failed to be
184 secreted. Based on the mannose content in the cell wall fractions compared with WT, the
185 amount of glucomannan inside cells was small. Interestingly, although the *man6* mutation
186 did not influence the glucomannan content alone, it enhanced this retention of
187 glucomannan in *man2-1 man5-1* (Fig. 3B). Given that AtMAN6 negatively regulates
188 secondary cell wall thickening as reported (28), the *man6* mutation might have positively
189 regulated the synthesis of secondary cell wall components including glucomannan
190 resulting in more aggregates inside cells. To identify such glucomannans retained inside
191 cells, immunoelectron microscopy was conducted. In this experiment, the glucomannans
192 in the ultrathin cross sections from the inflorescence stem of *man2-1 man5-1 man6-1*
193 were recognized by LM21 as the primary antibody and visualized with a secondary
194 antibody conjugated to gold particles. In the triple mutant, relatively large clusters of gold
195 particles were found in the vacuole (Fig. 3C). Although only as weak signals, such
196 clusters were also found in WT. Consistent with immunostaining and cell wall analysis,
197 there were fewer gold particles in the cell walls of the triple mutant, confirming the loss

198 of glucomannan in the cell walls.

199

200 **Tissue and subcellular localization of AtMAN2 and AtMAN6 differ**

201 The tissue and subcellular localization of AtMAN2 was investigated using transgenic
202 Arabidopsis harboring *pMAN2::MAN2TM-mNeon* in which the fluorescent protein
203 mNeonGreen sequence was inserted right behind the TM domain in the genomic *AtMAN2*
204 sequence (Fig. S6). To compare, we also generated *pMAN6::MAN6signal-mNeon* in
205 which the mNeonGreen sequence was inserted after the signal peptide into the genomic
206 *AtMAN6* sequence. In this experiment, the top part of the inflorescence stem was chosen
207 for observation because we found strong mNeonGreen signals there. The MAN2TM-
208 mNeon signal was widely observed in the vascular and fiber cells of inflorescence stems
209 (Fig. 4A-I), and this was substantially different from MAN6signal fluorescence, which
210 was limited to developing vessels (Fig. 4J-R, S6). The MAN2TM-mNeon signal was
211 localized in the Golgi apparatus, suggesting that AtMAN2 functions in the Golgi
212 apparatus. The MAN6signal fluorescence were spread in the vessel cells, indicating its
213 localization in the ER or the vacuole. C-terminal fusion of AtMAN6 with green
214 fluorescence protein has been used previously to show that AtMAN6 localizes on the
215 plasma membrane (PM), but in that study, as in this, AtMAN2 and AtMAN6 were found
216 in substantially different locations, suggesting that they have different molecular
217 functions (29).

218

219 # DISCUSSION

220 **MANs are novel factors necessary for glucomannan synthesis**

221 The present study has identified AtMAN2 and AtMAN5 as factors necessary for normal
222 glucomannan synthesis in Arabidopsis, to work along with VTC1 and KJC1 generating
223 GDP-Man, CslAs catalyzing the glucomannan backbone synthesis, and MSRs (12, 14-16,
224 20). Based on the distribution of orthologues, it is likely that many angiosperms utilize
225 TM-type MANs in glucomannan synthesis.

226 The requirement of polysaccharide degrading enzymes for polysaccharide synthesis
227 presents an apparent paradox. Yet this is not the first example: among other plant
228 glycoside hydrolases, the membrane-associated GH9 endo-β-1,4-glucanase
229 KORRIGAN1 (KOR1) is well known for its role in cellulose synthesis (33). The
230 Arabidopsis *kor1* mutant suffers severe defects in the synthesis of cellulose,
231 demonstrating the importance of this protein. The sea squirt *Ciona intestinalis* and
232 bacteria such as *Agrobacterium tumefaciens* and *Acetobacter xylinum* also require endo-
233 β-1,4-glucanases for their cellulose synthesis. These enzymes belong to the GH 6 and 8
234 families and are thus distinct from KOR1 (34-36). These facts imply that hydrolytic
235 activity of endo-β-1,4-glucanases is important to facilitate the cellulose synthesis. The
236 present study describes an instance of another version of this paradox in polysaccharide
237 synthesis, after the case of endo-β-1,4-glucanase in cellulose synthesis. We suggest that
238 this paradox may represent a general mechanism in plant cells to prevent the aggregation
239 of newly synthesized cell wall polysaccharides.

240

241 **Putative molecular functions of AtMAN2 and AtMAN5**

242 Previous research has shown that AtMAN2 lacks transglycosylation activity (30).
243 MAN2TM-mNoen localizes in the Golgi apparatus in the vascular and interfascicular
244 fiber cells (Fig. 4). Based on these facts, we suggest that glucomannan probably
245 undergoes hydrolysis rather than transglycosylation by AtMAN2 and AtMAN5 in the
246 Golgi apparatus. The drastic decrease in the glucomannan content in the double and triple
247 mutants implies that the synthesis by CslAs nearly stops. The alternative, that only
248 secretion is impaired in the mutants, while the glucomannan synthesis by CslA2 and
249 CslA9 is maintained, does not seem likely, because in this case the glucomannan must
250 have been collected in any fraction (Fig. 2B). We cannot specify the molecular functions
251 of these MANs in detail, but it is conceivable that large glucomannan molecules before
252 decoration easily aggregate during synthesis, which may cause the chain elongation
253 reaction by CslAs to stop. This problem may be alleviated through partial hydrolysis by
254 these MANs. It is also probable that AtMAN2 and AtMAN5 facilitate the release of
255 glucomannan from CslA proteins by partial hydrolysis during synthesis, enabling its
256 proper loading into the secretion pathway. The impairment of this process may slow down
257 or stop the glucomannan synthesis by CslAs and result in the formation of aggregates that
258 are transported to the vacuole.

259 Another atypical MAN, AtMAN6, has been reported to negatively regulate secondary
260 cell wall thickening by localizing to the plasma membrane and releasing oligosaccharides
261 from cell wall glucomannan as signaling molecules (28, 29). The different impacts on the
262 glucomannan content and subcellular localization strongly suggest that AtMAN2 and

263 AtMAN5 play roles distinct from AtMAN6. The clear functional differences, despite their
264 high sequence similarity, between secreted MANs, MAN2/MAN5, and MAN6 highlight
265 the complexity of glucomannan synthesis and degradation processes in plants.
266
267 **Transport of glucomannan to the vacuole**
268 Undecorated hemicellulose polysaccharides such as xyloglucan, xylan, and mannan
269 polysaccharides tend to form insoluble aggregates due to the straight ribbon-like structure
270 of their backbones, which is suitable for intermolecular interaction. In xyloglucan, the
271 importance of galactose-side chains to avoid aggregation has been shown (37-39). The
272 Arabidopsis *murus3* (*mur3*) mutant, which lacks galactose-side chains on its xyloglucan,
273 suffers intracellular aggregation of xyloglucan in the roots, resulting in growth defects. In
274 this case, the aggregates likely accumulated in the Golgi apparatus leading to the
275 disruption of cellular trafficking in young tissues. However, the defects caused by *man2*
276 and *man5* mutations differ from those observed for *mur3* mutants. First, the *man* mutants
277 did not show any growth defects, suggesting that AtMAN2 and AtMAN5 are more
278 important in the formation of secondary cell walls than in the formation of the primary
279 cell walls. Second, the glucomannan was retained in the vacuole, which was also observed
280 in WT to a lesser extent in our previous study (Fig. 3) (40). Therefore, the transport of
281 glucomannan to the vacuole is likely a normal reaction to avoid serious disruption of
282 intracellular trafficking in tissue rapidly synthesizing hemicellulose for secondary cell
283 walls. Thus, plant cells likely have a transport route to deliver cell wall polysaccharides
284 to the vacuole not to the cell walls (41). Clarifying this mechanism will presumably

285 require the identification of as yet unknown factors involved in this transport.

286

287 # MATERIALS AND METHODS

288 **Arabidopsis mutants and growth conditions**

289 *Arabidopsis thaliana* ecotype Col-0 was used in this study. The T-DNA insertion lines
290 SALK_0383344 (*man2-1*), SALK_016450 (*man2-2*), SALK_059047 (*man5-1*), and
291 SALK_129977 (*man6-1*) were provided by the Arabidopsis Biological Resource Center.
292 The double and triple mutants were generated by crosses between these mutants. The
293 genotypes of the mutants were determined using specific primers (Fig. S7 and Table S1).
294 The *csla2-2 csla9-2* and *msr1-1 msr2-1* double mutants had been obtained in our previous
295 studies (14, 20, 42). Arabidopsis seeds were sterilized and sown on Murashige and Skoog
296 (MS) medium in 0.8% (w/v) agar. After stratification at 4 °C in the dark for 2 days, the
297 seeds were germinated and grown under continuous light (cold cathode fluorescent lamp;
298 Biomedical Science) at 23 °C for 10 days, then on rockwool fiber for 4 weeks under
299 continuous light at 23 °C.

300

301 **Phylogenetic analysis**

302 The amino acid sequences of MANs from various plants were collected using Basic Local
303 Alignment Search Tool in NCBI (https://blast.ncbi.nlm.nih.gov/Blast.cgi) (Table S2). The
304 signal peptide and transmembrane region were detected using the SignalP 6.0 and
305 TMHMM-2.0 programs, respectively (43-45). The alignments of amino acid sequences
306 were performed by the MUSCLE program in MEGA software (version 11; 46) with

307 default parameters. The phylogenetic trees were generated using the maximum likelihood
308 method with 100 bootstraps.
309
310 **Cell wall fractionation and sugar composition analysis**
311 The bottom part of first inflorescence stem 2 weeks after bolting (approximately 50 mg)
312 was homogenized with mortar and pestle in water (Fig. S8). After centrifugation at 10,000
313 x g at 4°C for 5 min, the supernatant was collected as the soluble fraction. The precipitate
314 was suspended in 0.4 mL of 4 M potassium hydroxide containing 0.04% (w/v) $NaBH_4$ at
315 25°C. After centrifugation at 10,000 x g at 4 °C for 5 min, the supernatant was collected.
316 This extraction was repeated. The combined supernatant (0.8 mL) was neutralized with
317 0.4 mL of glacial acetic acid and collected as the alkali fraction. The precipitate was
318 washed with 98% (v/v) ethanol, 2% (v/v) acetic acid twice, lyophilized for 24 h,
319 hydrolyzed with 72% (v/v) sulfuric acid at 4 °C for 1 h and 8% (v/v) sulfuric acid at
320 100 °C for 4 h, and then collected as the cellulose fraction. Total sugar composition and
321 quantity of the above fractions were determined using the phenol sulfuric acid procedure
322 (47).
323 For sugar composition analysis, the alkali fraction was dialyzed against water at 4 °C
324 for 2 days. The soluble and alkali fractions were hydrolyzed into monosaccharides with
325 2 M trifluoroacetic acid (TFA) at 121 °C for 1 h, then lyophilized to remove TFA. The
326 cellulose fraction after the hydrolysis with sulfuric acid was neutralized with barium
327 carbonate and desalted with Dowex beads (Dowex 50WX8, Dow Chemical).
328 Monosaccharide composition was determined by HPAEC-PAD using a Dionex ICS-

329 5000+ liquid chromatograph (Thermo Fisher Scientific) fitted with a CarboPac PA-1
330 column (Thermo Fisher Scientific) and a pulsed amperometric detector (Thermo Fisher
331 Scientific) as described previously (15).
332
333 **PACE**
334 Alcohol-insoluble residue (AIR) was prepared from the bottom part of Arabidopsis
335 inflorescence stems (fresh weight, 100 mg) according to Yu et al. (7). Glucomannans were
336 extracted from the AIR with 1 mL of 4 M potassium hydroxide solution by shaking at
337 1,000 rpm at room temperature for an hour. After centrifugation at 15,000 x g for 15
338 minutes, the supernatant was collected. To collect remaining glucomannans, the pellet
339 was suspended in 1 mL of water. After centrifugation, the supernatant was collected. The
340 supernatants were combined and applied to a PD-10 column (Cytiva) to exchange the
341 solvent with 50 mM ammonium acetate buffer (pH 6.0). The eluted fraction was used as
342 the KOH fraction.
343 Glucomannans in the KOH fraction were hydrolyzed into specific oligosaccharides
344 with a commercial endo-β-1,4-mannanase, CjMan26A (1 unit, E-BMACJ, Megazyme),
345 from *Cellvibrio japonicus* in 50 mM ammonium acetate buffer (pH 6.0) at 37 °C
346 overnight (Fig. S4). After the reaction, the enzyme was denatured by heating at 100 °C
347 for 15 minutes. The oligosaccharides were derivatized with 8-aminonapthalene-1,3,6-
348 trisulphonic acid, resuspended in urea, and separated by electrophoresis as described (6,
349 14). Gels were visualized using a G-Box (Syngene, Cambridge, UK) with a

350 transilluminator with long-wave tubes emitting at 365 nm and a shortpass (500 to 600
351 nm) detection filter. Mannose and β-1,4-mannooligosaccharides (Man_{2-6}, Megazyme)
352 were used as standards.
353
354 **Immunostaining of glucomannan in the mutants**
355 The glucomannan and xylan in the inflorescence stems were observed using specific
356 antibodies. The bottom part of inflorescence stems (the lowest one-sixth portion) was
357 fixed with 4% (v/v) paraformaldehyde and 0.6% (v/v) glutaraldehyde at 4 °C for 3 h. The
358 fixed samples were dehydrated through a graded ethanol series, embedded in Technovit
359 7100 (Nisshin EM, Tokyo, Japan) using a graded series of ethanol and Technovit 7100
360 mixtures, and solidified with Technovit hardener (Nisshin EM) at 60 °C for 12 h. Sections
361 were sliced to a thickness of 10 μm using a microtome (RM2125RT; Leica, Tokyo, Japan)
362 equipped with a disposable steel blade (C35; Feather, Osaka, Japan).
363 To remove acetyl groups from polysaccharides, the cross-sections were treated with 50
364 mM NaOH at 25 °C for 30 min. The sections were then washed with phosphate-buffered
365 saline (PBS) containing 137 mM NaCl, 10 mM Na_2HPO_4, 2.7 mM KCl, and 1.8 mM
366 KH_2PO_4 (pH 7.4) and then blocked in PBS containing 0.3% (w/v) blocking milk (Sigma-
367 Aldrich, Tokyo, Japan) for 30 min. Then, the sections were incubated for 1.5 h with
368 antibodies against glucomannan (LM21, Kerafast, Shirley, MA; dilution 1:5) or xylan
369 (LM10, Kerafast; dilution 1:5) in PBS with blocking milk. After washing three times with
370 PBS, the sections were incubated for 1 h with Alexa Fluor 488-conjugated anti-mouse
371 IgM for LM21 (abcam, Cambridge, UK; dilution 1:100) or Alexa Fluor 488-conjugated

372 anti-mouse IgG for LM10 (abcam; dilution 1:100) in PBS with bovine serum albumin.
373 The sections were washed three additional times with PBS.
374 The cross sections were imaged with a microscope (ECLIPSE Ci-L Plus, Nikon, Japan)
375 at 405 nm for Calcofluor White and at 488 nm for specific antibodies.
376
377 **Immunoelectron microscopy**
378 Immunoelectron microscopy to detect the glucomannan localization was performed
379 according to Atsuzawa et al. (48). The bottom part (the lowest one-sixth portion) and
380 upper part (the highest one-sixth portion) of the inflorescence stems of WT and the *man2-*
381 *1 man5-1 man6-1* mutant were fixed with 2% (v/v) gultaraldehyde in 50 mM potassium
382 phosphate (pH 6.8) at room temperature for 3 h. After washing with 100 mM lysine in 50
383 mM potassium phosphate (pH 6.8) the samples were dehydrated in a graded series of
384 ethanol. The tissues were embedded in LR White resin (Electron Microscopy Sciences,
385 USA) and polymerized by heating at 60 °C. Ultrathin sections of 100 nm thickness were
386 cut on an UltracutN ultramicrotome (Nissei, Japan) and collected on nickel grids coated
387 with polyvinyl formvar membrane.
388 Ultra-thin sections were immersed in 50 mM NaOH at room temperature for 30 min
389 and washed with Tris-HCl buffer (TBS: 50 mM Tris-HCl (pH 7.5), 150 mM NaCl,)
390 containing 0.05% Triton X-100 (TBS/Tx). They were treated with blocking solution (10
391 mg/ml bovine serum albumin in TBS) at room temperature for 60 min, and they were
392 incubated with LM21 antibody at 1:500 dilution at 4 °C overnight. After washing with

393 TBS/Tx, the sections were incubated with a solution of 10 nm gold particles conjugated
394 with goat anti-rat IgG (BBI solutions, UK) as the secondary antibody at a 1:30 dilution
395 for 1 h at room temperature and washed with TBS/Tx. Specimens were observed with a
396 transmission electron microscope (H-7500, Hitachi, Japan) at an accelerating voltage of
397 80 kV after staining with uranyl acetate and lead citrate.
398
399 **Transgenic plants expressing MAN-mNeonGreen**
400 The DNA fragments of *genomic AtMAN2 and AtMAN6* genes and mNeonGreen were
401 amplified from Arabidopsis genomic DNA and template *mNeonGreen* (Addgene,
402 #189976), respectively, using the primer sets listed in Table S1. The DNA fragments were
403 assembled and subcloned into the binary vector pBGGN (Inplanta Innovation, Yokohama,
404 Japan) with DNA assembly kit (Gibson) to yield the constructs, *pMAN2::MAN2TM-*
405 *mNeon/pBGGN* and *pMAN6::MAN2signal-mNeon/pBGGN* (Fig. S6). These constructs
406 were introduced into the *man2-1 man5-1 man6-1* triple mutants by an Agrobacterium-
407 mediated (*Rhizobium radiobacter*, EHA105 strain) method (49).
408
409 **Observation of tissue and subcellular localization of MAN-mNeonGreen proteins**
410 Cross sections were excised from the top part of the inflorescence stems of the transgenic
411 plants harboring *pMAN6::MAN2signal-mNeon* (line #3) or *pMAN6::MAN2signal-mNeon*
412 (line #3) and stained with 6.34 μM fixable analog of N-(3-triethylammoniumpropyl)-4-
413 (6-(4-(diethylamino) phenyl) hexatrienyl) pyridinium dibromide, FM 4-64FX
414 (ThermoFisher). The confocal images were obtained using a Zeiss LSM800 (Zeiss, Jena,

Germany) with a Plan-Apochromat 63×/1.4 oil immersion objective lens. FM 4-64FX was excited at 561 nm and detected between 400 and 645 nm. Fluorescence signals from mNeonGreen were detected after excitation at 488 nm and detected between 410-546 nm. Autofluorescence was excitated at 488 nm and detected at 550-700 nm. Transmitted photomultiplier tube (T-PMT) images were also captured during confocal imaging.

Author Contributions: T.K. and P.D. designed the research. A.K., E.S., Y.Y., H.T., N.N., K.A., Y.K., D.T., and T.K. performed research. E.S., Y.Y., D.T., Y.K., and T.K. analyzed the data. H.T., Y.K., D.T., P.D., and T.K. wrote the manuscript.

Conflict of interest

The authors declare no conflict of interest.

Acknowledgments: We thank Dr. Kiminori Toyooka from RIKEN and Prof. Masatsugu Toyota from Saitama University for valuable discussions. This work was supported by MEXT KAKENHI Grant-in-Aid for Scientific Research to T. Kotake [no. 18H05495], Grant-in-Aid for Scientific Research to T. Kotake [no. 23H04302, and no. 23H02134] and to D. Takahashi [no. 23K05144], the ERC Advanced Grant EVOCATE to P. Dupree funded by the United Kingdom Research and Innovation (UKRI) grant number EP/X027120/1 (www.ukri.org) and by the grant OpenPlant (UKRI BBSRC, BB/L014130/1) to P. Dupree, and a Broodbank Research Fellowship to Y. Yoshimi (reference no. PD16178).

437

438 ## Supporting Information

439 **Table S1.** Primers used for genotyping and plasmid construction.

440 **Table S2.** List of MAN sequences in the phylogenetic analysis.

441

442 **Fig. S1.** Growth phenotypes of *man* mutants

443 **Fig. S2.** Expression patterns of *AtMAN2*, *AtMAN5*, and *AtMAN6* genes.

444 **Fig. S3.** Monosaccharide composition of the soluble, alkali, and cellulose fractions.

445 **Fig. S4.** Oligosaccharides detected by PACE.

446 **Fig. S5.** Glucomannan and xylan accumulation in *man* mutants.

447 **Fig. S6.** Transgenic plants expressing MAN2TM-mNeon and MAN6signal-mNeon.

448 **Fig. S7.** T-DNA insertion sites and genotyping of man mutants.

449 **Fig. S8.** Cell wall fractionation from inflorescence stems.

450

LITERATURE CITED

1. **Y. M. Bar-On, R. Phillips, R. Milo,** The biomass distribution on Earth. *Proc. Natl. Acad. Sci. U.S.A.* **115**, 6506-6511 (2018).
2. **J. Verbančič, J. E. Lunn, M. Stitt, S. Persson,** Carbon supply and the regulation of cell wall synthesis. *Mol. Plant* **11**, 75-94 (2018).
3. **K, Mori,** Tripartite management of unfolded proteins in the endoplasmic reticulum. *Cell* **5**, 451-454 (2000).

4. **H. V. Scheller, P. Ulvskov,** Hemicelluloses. *Annu. Rev. Plant Biol.* **61**, 263-289 (2010).
5. **C. Voiniciuc,** Modern mannan: a hemicellulose's journey. *New Phytol.* **234**, 1175-1184 (2022).
6. **Y. Yoshimi *et al.*,** Glucomannan engineering highlights the role of galactosyl modification in fine-tuning cellulose-glucomannan interaction in Arabidopsis cell walls. *Nat. Commun*. (2025) doi.org/.
7. **L. Yu *et al.*,** The patterned structure of galactoglucomannan suggests it may bind to cellulose in seed mucilage. *Plant Physiol* **178**, 1011-1026 (2018).
8. **L. Yu L *et al.*,** Eudicot primary cell wall glucomannan is related in synthesis, structure, and function to xyloglucan. *Plant Cell* **34**, 4600-4622 (2022).
9. **H. D., Chanzy, A., Grosrenaud, R., Vuong, W., Mackie,** The crystalline polymorphism of mannan in plant cell walls and after recrystallisation. *Planta* **161**, 320-329 (1984).
10. **Y. Zhou, R. Jiang, W. S. Perkins, Y. Cheng,** Morphology evolution and gelation mechanism of alkali induced konjac glucomannan hydrogel. *Food Chem.* **269**, 80-88 (2018).
11. **K. S. Dhugga *et al.*,** Guar seed beta-mannan synthase is a member of the cellulose synthase super gene family. *Science* **303**, 363-366 (2004). doi: 10.1126/science.1090908.
12. **P. L. Conklin *et al.*,** Genetic evidence for the role of GDP-mannose in plant ascorbic acid (vitamin C) biosynthesis. *Proc. Natl. Acad. Sci. U.S.A.* **96**, 4198–4203 (1999).
13. **A. H. Liepman, C. G. Wilkerson, K. Keegstra,** Expression of cellulose synthase-like (Csl) genes in insect cells reveals that CslA family members encode mannan synthases. *Proc. Natl. Acad. Sci. U.S.A.* **102**, 2221-2226 (2005).
14. **F. Goubet *et al.*,** Cell wall glucomannan in Arabidopsis is synthesised by CSLA glycosyltransferases, and influences the progression of embryogenesis. *Plant J.* **60**, 527-538 (2009).
15. **S. Sawake *et al.*,** KONJAC1 and 2 are key factors for GDP-mannose generation and affect L-ascorbic Acid and glucomannan biosynthesis in Arabidopsis. *Plant Cell* **27**, 3397-3409 (2015).
16. **N. Nishigaki *et al.*,** Galactoglucomannan structure of Arabidopsis seed-coat mucilage

490 in GDP-mannose synthesis impaired mutants. *Physiol. Plant.* **173**, 1244-1252 (2021).
491 **17. J. S. Reid, M. E. Edwards, C. A. Dickson, C. Scott, M. J. Gidley,** Tobacco
492 transgenic lines that express fenugreek galactomannan galactosyltransferase
493 constitutively have structurally altered galactomannans in their seed endosperm cell
494 walls. *Plant Physiol.* **131**, 1487-1495 (2003).
495 **18. C. Voiniciuc *et al.*,** MUCILAGE-RELATED10 produces galactoglucomannan that
496 maintains pectin and cellulose architecture in Arabidopsis seed mucilage. *Plant*
497 *Physiol.* **169**, 403-420 (2015).
498 **19. R. Zhong, D. Cui, Z. H. Ye,** Members of the DUF231 family are O-acetyltransferases
499 catalyzing 2-O- and 3-O-acetylation of mannan. *Plant Cell Physiol.* **59**, 2339-2349
500 (2018).
501 **20. Y. Wang *et al.*,** Identification of an additional protein involved in mannan biosynthesis.
502 *Plant J.* **73**, 105-117 (2013).
503 **21. H. Aspeborg, P. M. Coutinho, Y. Wang, H. Brumer 3rd, B. Henrissat,** Evolution,
504 substrate specificity and subfamily classification of glycoside hydrolase family 5
505 (GH5). *BMC Evol. Biol.* **12**, 186 (2021).
506 **22. R. Schröder, T.F. Wegrzyn, K.M. Bolitho, R.J. Redgwell RJ,** Mannan
507 transglycosylase: a novel enzyme activity in cell walls of higher plants. *Planta* **219**,
508 590-600.
509 **23. R. Iglesias-Fernández, M.C. Rodríguez-Gacio, C. Barrero-Sicilia C, P.**
510 **Carbonero, A. Matilla,** Three endo-β-mannanase genes expressed in the micropylar
511 endosperm and in the radicle influence germination of *Arabidopsis thaliana* seeds.
512 *Planta* **233**, 25-36 (2011).
513 **24. Y. Wang, F. Vilaplana, H. Brumer, H. Aspeborg,** Enzymatic characterization of a
514 glycoside hydrolase family 5 subfamily 7 (GH5_7) mannanase from Arabidopsis
515 thaliana. *Planta* **239**, 653-665 (2014).
516 **25. J. Chen *et al.*,** MAN3 gene regulates cadmium tolerance through the glutathione-
517 dependent pathway in Arabidopsis thaliana. *New Phytol.* **205**, 570-582 (2015).
518 **26. Q. Wu, Y. T. Meng, Z. H. Feng, R. F. Shen, X. F. Zhu,** The endo-β-mannase MAN7
519 contributes to cadmium tolerance by modulating root cell wall binding capacity in
520 *Arabidopsis thaliana*. *J. Integr. Plant Biol.* **65**, 1670-1686 (2023).
521
522
523 **27. J.C. Alvim *et al.*,** The K/HDEL receptor does not recycle but instead acts as a Golgi-
524 gatekeeper. *Nat. Commun.* **14**, 1612 (2023).
525 **28. Y. Zhao, D. Song, J. Sun, L. Li,** Populus endo-β-mannanase PtrMAN6 plays a role
526 in coordinating cell wall remodeling with suppression of secondary wall thickening
527 through generation of oligosaccharide signals. *Plant J.* **74**, 473-85 (2013).
528 **29. R. Zhang, B. Li, Y. Zhao, Y. Zhu, L. Li,** An essential role for mannan degradation
529 in both cell growth and secondary cell wall formation. *J. Exp. Bot.* **75**, 1407-1420

530 (2023).
531 **30. Y. Wang *et al.*,** Biochemical characterization of the novel endo-beta-mannanase
532 AtMan5-2 from *Arabidopsis thaliana*. *Plant Sci.* **241**, 151-163 (2015).
533 **31. D. Winter *et al.*,** An "Electronic Fluorescent Pictograph" browser for exploring and
534 analyzing large-scale biological data sets. *PLoS One* **2**, e718 (2007).
535 **32. D. Mohnen,** Pectin structure and biosynthesis. *Curr. Opin. Plant Biol.* **11**, 266-277
536 (2008).
537 **33. F. Nicol et al.,** A plasma membrane-bound putative endo-1,4-beta-D-glucanase is
538 required for normal wall assembly and cell elongation in Arabidopsis. *EMBO J.* **17**,
539 5563-5576 (1998).
540 **34. R. Standal *et al.*,** A new gene required for cellulose production and a gene encoding
541 cellulolytic activity in *Acetobacter xylinum* are colocalized with the *bcs* operon. *J.*
542 *Bacteriol.* **176**, 665–672 (1994).
543 **35. A. G. Matthysse, S. White, R. Lightfoot,** Genes required for cellulose synthesis in
544 Agrobacterium tumefaciens. *J. Bacteriol.* **177**, 1069-1075 (1995).
545 **36. K. L. Li, K. Nakashima, K. Hisata, N. Satoh,** Expression and possible functions of
546 a horizontally transferred glycosyl hydrolase gene, GH6-1, in Ciona embryogenesis.
547 *Evodevo* **14**, 11 (2023).
548 **37. K. Tamura, T. Shimada, M. Kondo, M. Nishimura, I. Hara-Nishimura,**
549 KATAMARI1/MURUS3 is a novel golgi membrane protein that is required for
550 endomembrane organization in Arabidopsis. *Plant Cell* **17**, 1764-1776 (2005).
551 **38. Y. Kong *et al.*,** Galactose-depleted xyloglucan is dysfunctional and leads to dwarfism
552 in Arabidopsis. *Plant Physiol.* **167**, 1296-306. doi: 10.1104/pp.114.255943 (2015).
553 **39. N. Hoffmann, H. E. McFarlane,** Xyloglucan side chains enable polysaccharide
554 secretion to the plant cell wall. *Dev. Cell* **59**, 2609-2625.e8. doi:
555 10.1016/j.devcel.2024.06.006.
556 **40. M. G. Handford *et al.*,** Localisation and characterisation of cell wall mannan
557 polysaccharides in Arabidopsis thaliana. *Planta* **218**, 27-36. doi: 10.1007/s00425-
558 003-1073-1079.
559 **41. K. Herburger, S. Głazowska, J. Mravec,** Bricks out of the wall: polysaccharide
560 extramural functions. *Trends Plant Sci.* **27**, 1231-1241 (2022).
561 **42. F. Goubet, P. Dupree P, K. S. Johansen,** Carbohydrate gel electrophoresis. *Methods*
562 *Mol. Biol.* **715**, 81-92.
563 **43. F. Teufel *et al.*,** SignalP 6.0 predicts all five types of signal peptides using protein
564 language models. *Nat. Biotechnol.* **40**, 1023-1025 (2022).
565 **44. A. Krogh, B. Larsson, G. von Heijne, E. L. Sonnhammer,** Predicting
566 transmembrane protein topology with a hidden Markov model: application to
567 complete genomes. *J. Mol. Biol.* **305**, 567-580. doi: 10.1006/jmbi.2000.4315 (2001).
568 **45. S. Möller S, M. D. Croning MD, R. Apweiler R,** Evaluation of methods for the
569 prediction of membrane spanning regions. *Bioinformatics* **17**, 646-653 (2001).
570 **46. K. Tamura, G. Stecher, S. Kumar,** MEGA11: Molecular Evolutionary Genetics

Analysis version 11. *Mol. Biol. Evol.* **38**, 3022-3027 (2021).

47. **M. Dubois, K. A. Gilles, J. K. Hamilton, P. A. Rebers, F. Smith,** Colorimetric method for determination of sugars and related substances. *Anal. Chem.* **28**, 350-356 (1956). doi: 10.1021/ac60111a017
48. **K. Atsuzawa *et al.*,** Immunohistochemical localization of mitochondrial fatty acid β-oxidation enzymes in Müller cells of the retina. *Histochem. Cell. Biol.* **134**, 565-579.
49. **S. J. Clough, A. F. Bent,** Floral dip: a simplified method for Agrobacterium-mediated transformation of Arabidopsis thaliana. *Plant J.* 16, 735-743 (1998).

584 **FIGURE LEGENDS**

585 **Figure 1. Distribution of TM-type MANs in plants.**

586 (A) Schematic model of AtMAN proteins. The signal peptide and transmembrane region
587 were identified by using SignalP 6.0 and TMHMM 2.0 programs, respectively. (B)
588 Phylogenetic tree of plant MANs. Phylogenetic relationships of MANs from Arabidopsis
589 and other plants including *S. moellendorffii*, *P. patens*, and *M. polymorpha* were analyzed
590 with MEGA software (version 11.0). Rice OsMAN5 and poplar PtrMAN6 indicated with
591 pink dots have HHEL and HDDL sequences at the C-terminus instead of HDEL,
592 respectively. SmMAN2 with the orange dot has a TM domain in the N-terminal region
593 that its neighbor, SmMAN3, lacks. MAN sequences from angiosperms are shown in black
594 whereas those from other organisms are in blue. Amt, amborella; Lj, *Lotus japonicus*; Mp,
595 *M. polymorpha*; Os, rice; Pp, *P. patens*; Sm, *S. moellendorffii*. AnMAN5A from
596 *Aspergillus nidulans* was used as the outgroup. Numbers in the nodes represent bootstrap
597 values. The bar indicates substitutions per site. The accession numbers and abbreviated
598 names for these sequences are listed in Table S2.

599

600 **Figure 2. Glucomannan content in *man* mutants.**

601 (A) Relative sugar content of cell wall fractions in the *man* mutants. Sugar content of
602 soluble, alkali, and cellulose fractions from the bottom part of inflorescence stems was
603 quantified by the phenol-sulfuric acid method. (B) Mannose content of cell wall fractions.
604 The content was calculated based on the sugar content and the monosaccharide
605 composition of cell wall fractions (Fig. S3). The values are shown in weight per gram

606 fresh weight (g fw). Data are mean values with standard deviation (three biological
607 replicates). Different letters indicate significant differences determined with the Tukey
608 HSD test ($p < 0.05$). (C) Change in β-GGM and AcGGM. GGMs included in the cell
609 walls of the bottom part of inflorescence stems were hydrolyzed into specific
610 oligosaccharides such as MGM, GBGM, $(GA)_2GM$ (Fig. S4), which were labelled with
611 a fluorescent compound then separated in the gel. Here, *man* mutants were compared with
612 WT, *csla2-2 csla9-2* double mutants known to lack stem glucomannans, and the *msr1-1*
613 *msr2-1* double mutant with reduced glucomannan (14, 20). The triple mutant #1, *man2-1*
614 *man5-1 man6-1*; the triple mutant #2, *man2-2 man5-1 man6-1*. Blue circle, glucose; green
615 circle, mannose; yellow circle, galactose. The oligosaccharide structures are shown on
616 the right. The results for control reactions are shown in Fig. S4.
617
618 **Figure 3. Glucomannan in the cell walls and the vacuole.**
619 (*A*) Reduced glucomannan in the inflorescence stem. Cross sections from the bottom part
620 of first inflorescence stem of *man* mutants were compared with WT. The images for bright
621 field, calcofluor staining, and glucomannan signals with LM21 antibody are shown. The
622 bar indicates 50 μm. (*B*) Magnified images of vascular cells. The merged images of
623 calcofluor staining, and glucomannan signals are shown. Arrowheads indicate relatively
624 strong glucomannan signals found inside cells. The bar indicates 10 μm. (*C*)
625 Representative images of immunoelectron microscopy. Ultrathin sections prepared from
626 the bottom and upper parts of the inflorescence stem of WT and the *man2-1 man5-1*
627 *man6-1* mutant were observed. Glucomannan was detected with LM21 antibody. The

628 gold particles found in the cell walls are shown as red dots and those in the cytoplasm
629 including the vacuole are represented as blue dots. CP, chloroplast; CW, cell wall; V,
630 vacuole. The bars indicate 1 μm.
631
632 **Figure 4. Tissue and subcellular localization of AtMAN2TM-mNeon and**
633 **AtMAN6signal-mNeon proteins in Arabidopsis.**
634 Vascular cells expressing MAN2TM-mNeon (A-I) and developing vessels expressing
635 MAN6signal-mNeon (J-R) in the top part of the inflorescence stem were observed with
636 a confocal microscope. Images for mNeonGreen (A, E, J, N), autofluorescence (B, F, K,
637 O), FM 4-64FX staining (G, P), and T-PMT (C, H, L, Q) were obtained and merged (D,
638 I, M, R). Scale bars are 100 μm in A-D and J-M and 5 μm in E-I and M-R. The
639 *pMAN2:MAN2TM-mNeon* and *pMAN6:MAN6signal-mNeon* constructs, the images of a
640 longitudinal section for AtMAN6signal-mNeon, and the recovery of the glucomannan
641 accumulation in *man2-1 man5-1 man6-1* with *pMAN2::MAN2TM-mNeon* are shown in
642 Fig. S6.
643

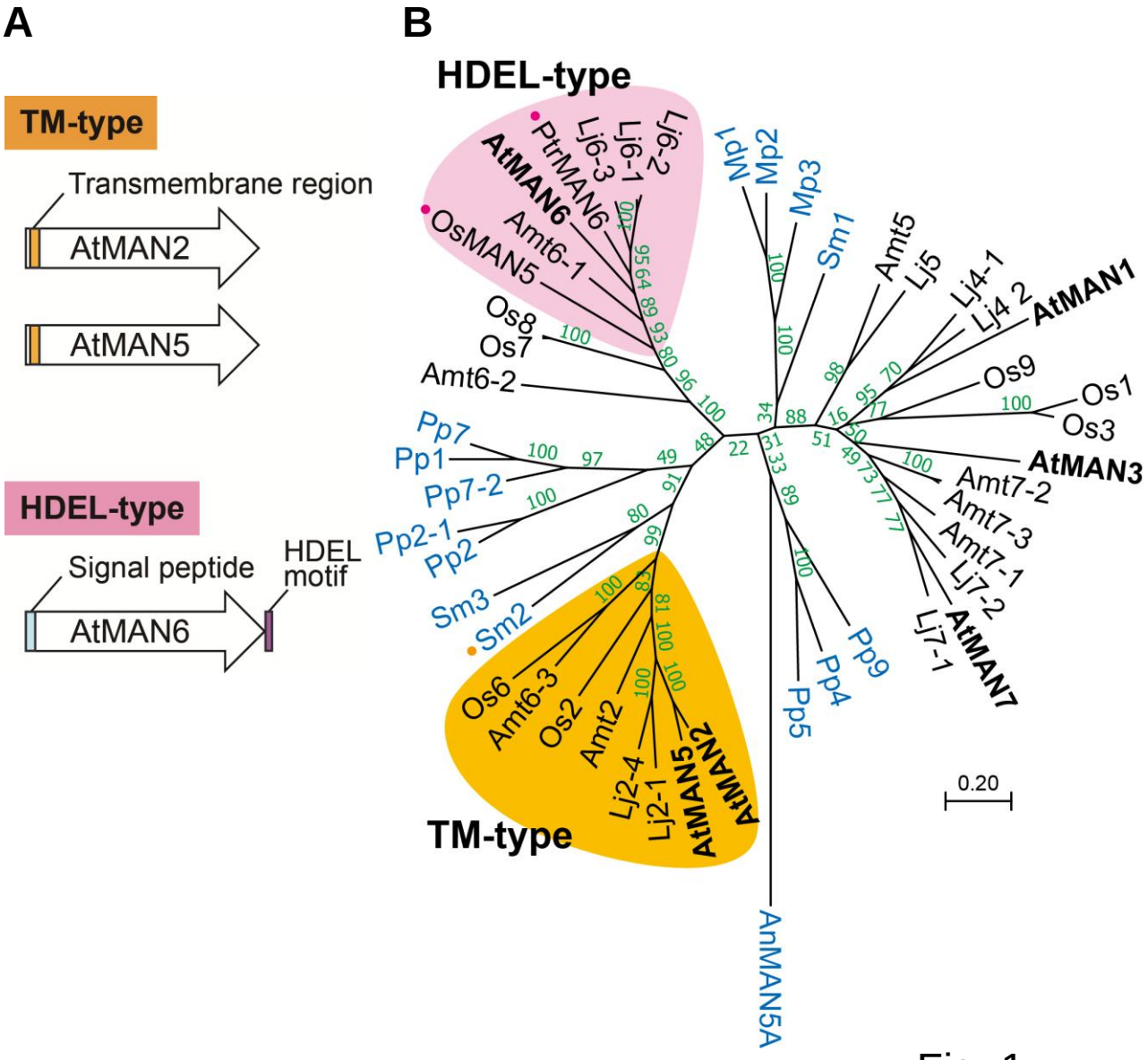
A
TM-type
Transmembrane region
AtMAN2
AtMAN5
HDEL-type
Signal peptide
HDEL motif
AtMAN6
B
HDEL-type
TM-type
Lj6-2
Lj6-1
Lj6-3
PtrMAN6
AtMAN6
OsMAN5
Amt6-1
Os8
Os7
Amt6-2
Mp1
Mp2
Mp3
Sm1
Amt5
Lj5
Lj4-1
Lj4 2
AtMAN1
Os9
Os1
Os3
AtMAN3
Amt7-2
Amt7-3
Amt7-1
Lj7-2
AtMAN7
Lj7-1
Pp9
Pp4
Pp5
Pp7
Pp1
Pp7-2
Pp2-1
Pp2
Sm3
Sm2
Os6
Amt6-3
Os2
Amt2
Lj2-4
Lj2-1
AtMAN5
AtMAN2
AnMAN5A
0.20

Fig. 1

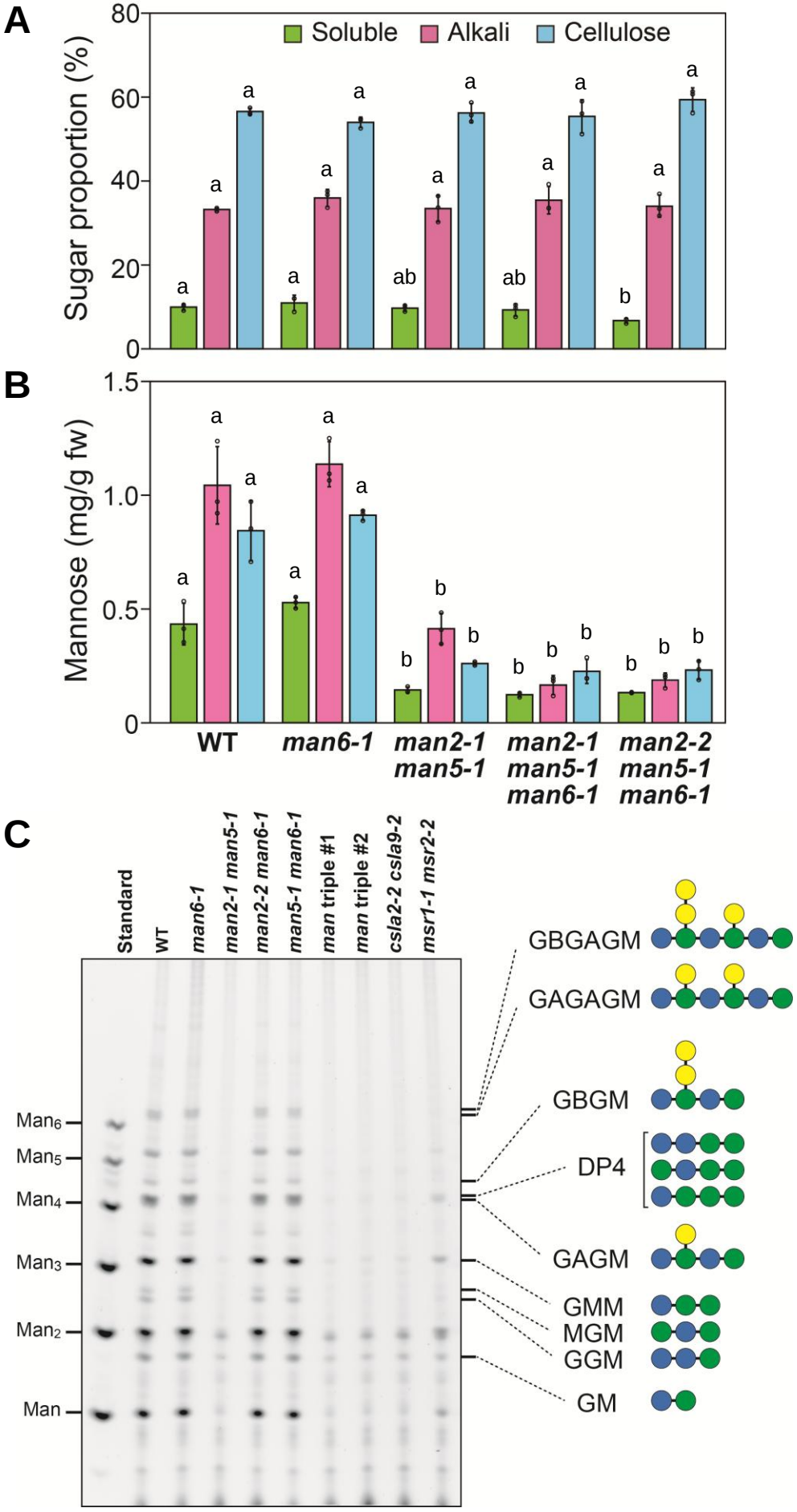
A
Soluble
Alkali
Cellulose
Sugar proportion (%)
80
60
40
20
0
B
Mannose (mg/g fw)
1.5
1.0
0.5
0
WT
man6-1
man2-1 man5-1
man2-1 man5-1 man6-1
man2-2 man5-1 man6-1
C
Standard
WT
man6-1
man2-1 man5-1
man2-2 man6-1
man5-1 man6-1
man triple #1
man triple #2
csla2-2 csla9-2
msr1-1 msr2-2
Man6
Man5
Man4
Man3
Man2
Man
GBGAGM
GAGAGM
GBGM
DP4
GAGM
GMM
MGM
GGM
GM

Fig. 2

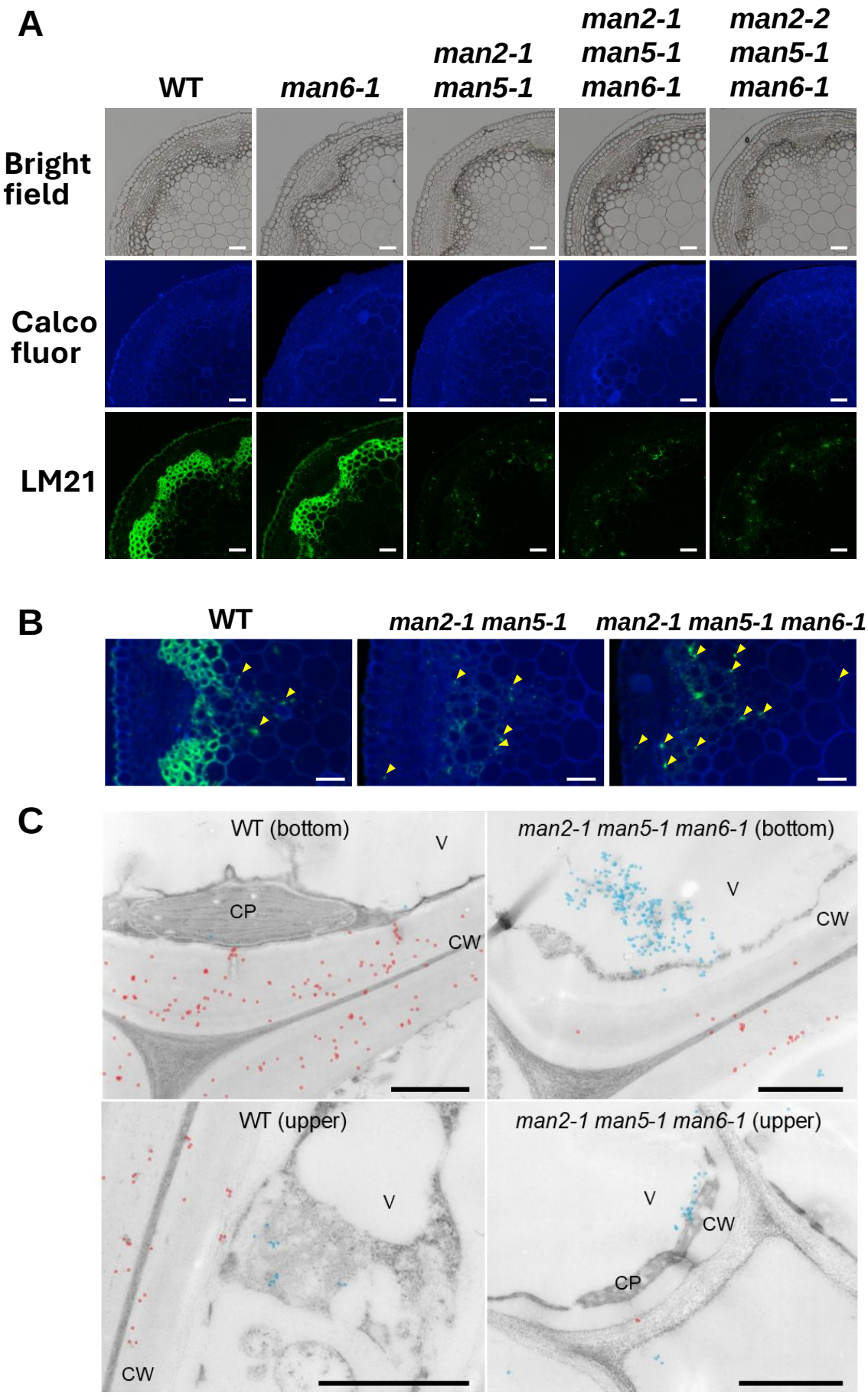
A
WT
man6-1
man2-1 man5-1
man2-1 man5-1 man6-1
man2-2 man5-1 man6-1
Bright field
Calco fluor
LM21
B
WT
man2-1 man5-1
man2-1 man5-1 man6-1
C
WT (bottom)
V
CP
CW
man2-1 man5-1 man6-1 (bottom)
V
CW
WT (upper)
V
CW
man2-1 man5-1 man6-1 (upper)
V
CW
CP

Fig. 3

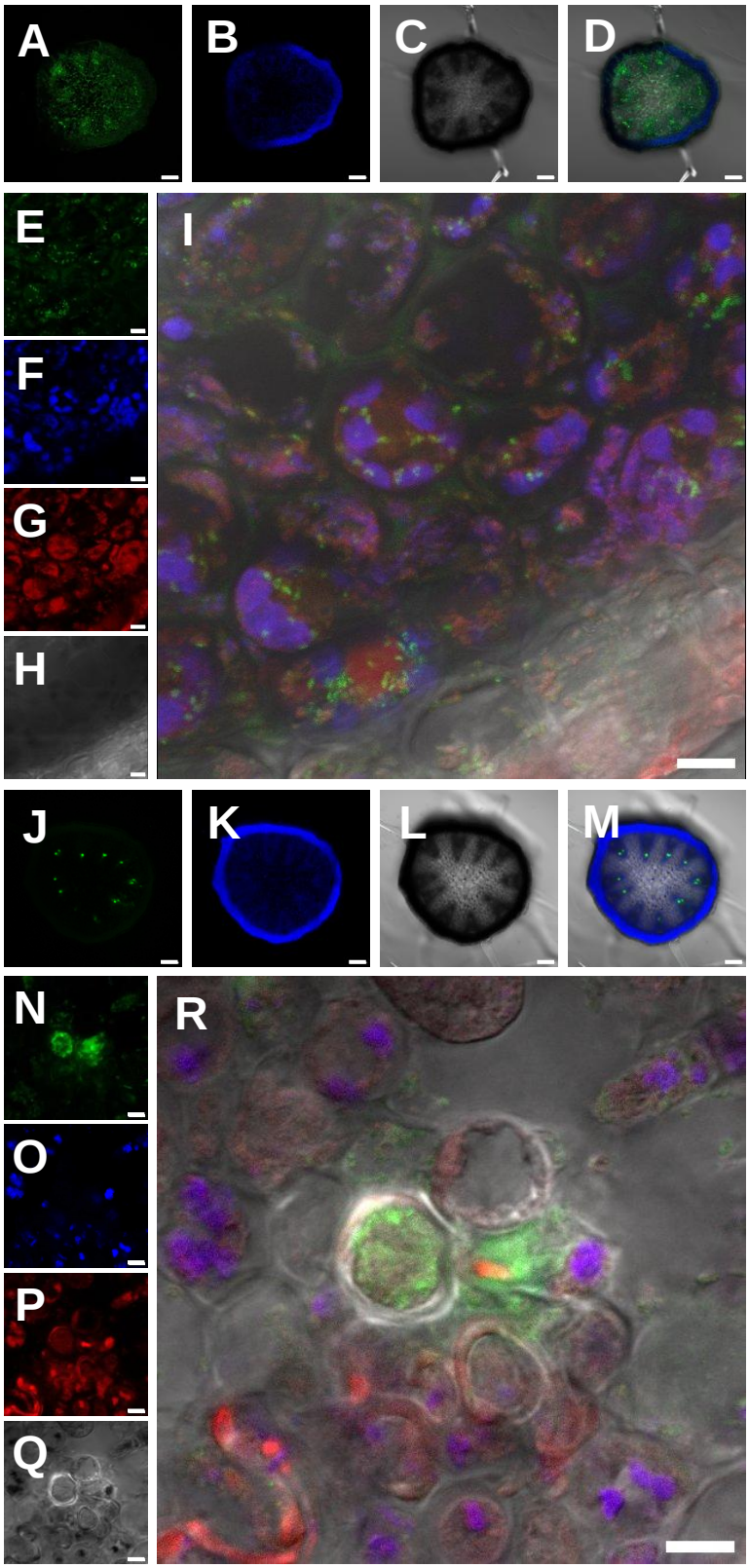

Fig. 4